

Contents lists available at [ScienceDirect](#)

## Journal of Marine Systems

journal homepage: [www.elsevier.com/locate/jmarsys](http://www.elsevier.com/locate/jmarsys)

## Do observations adequately resolve the natural variability of oceanic turbulence?

J.N. Moum <sup>a,\*</sup>, T.P. Rippeth <sup>b</sup>

<sup>a</sup> College of Oceanic & Atmos. Sci., Oregon State University, Corvallis, OR 97331-5503, USA

<sup>b</sup> School of Ocean Sciences, College of Natural Sciences, Bangor University, Menai Bridge, Anglesey, LL59 5AB, UK

### ARTICLE INFO

#### Article history:

Received 31 January 2008

Accepted 29 October 2008

Available online xxxx

#### Keywords:

Turbulence

Mixing

Review

### ABSTRACT

Especially in high Reynolds number, naturally-occurring flows, turbulence is a highly variable process. It is challenging to measure yet it is vital that we do so in order to quantify the internal transports of mass, nutrients, energy and momentum. Isolated turbulence profiles are difficult to interpret; systematic sampling and subsequent averaging are necessary. Confidence in our ability to properly sample turbulence arises from intergroup comparisons, comparisons with other methods to assess mixing coefficients and, most fundamentally, the constraints imposed by the governing fluid dynamics on both energy losses via viscous dissipation caused by turbulence and on the mixing that results from turbulence. Several examples in which fluid processes have been isolated from the full range of oceanic motions are reviewed in this light. These examples show how observationally-derived estimates of turbulence dissipation or mixing are consistent with larger scale constraints. The larger oceanographic problem of defining the full geographic variability of mixing remains.

© 2008 Elsevier B.V. All rights reserved.

### 1. Introduction

The detailed structure of turbulent flows defies prediction, yet the mechanics are not particularly complicated (Smyth and Moum, 2001). In fact we have learned considerably from detailed numerical simulations and laboratory experiments over the past several decades (e.g. Pope, 2000). In particular, a robust statistical description for stationary, homogeneous and isotropic turbulence has enabled our understanding of observed turbulent flows in terms of spectra, structure functions and/or probability density functions.

It is unlikely that turbulence in geophysical flows is ever stationary, homogeneous and isotropic, due to the modifications that arise from shear, stratification and the presence of boundaries. These factors are further complicated by the large Reynolds numbers ( $Re$ ) associated with geophysical flows. The range of motions that are excited in large  $Re$  flows con-

tributes to the intermittency (in time) and patchiness (in space) of turbulence (Thorpe, 2005). And it is rarely clear how to cleanly separate the sources of turbulence in field observations.

Given 1) these complications, 2) the geophysical deviations from the small  $Re$  experiments and simulations that the statistical descriptions are largely based, 3) measurement uncertainties and especially 4) the great natural intermittency that is apparent in any observation of geophysical turbulence, it is not unreasonable to ask how we can have confidence that our measurements of turbulence in the ocean are anything more than qualitative descriptors of the temporal and/or spatial variability of turbulence. We address this question with a summary of results that are not necessarily the most scientifically significant but rather contribute to our confidence that we do indeed understand how to quantify turbulence variables from our measurements, and to properly average these to yield dynamically important information. Our examples are to large extent based on personal experiences and not intended to be exhaustive. They are also, for the most part, restricted to cases where it is possible to isolate a particular fluid process. We hope

\* Corresponding author.

E-mail addresses: [moum@coas.oregonstate.edu](mailto:moum@coas.oregonstate.edu) (J.N. Moum), [t.p.rippeth@bangor.ac.uk](mailto:t.p.rippeth@bangor.ac.uk) (T.P. Rippeth).

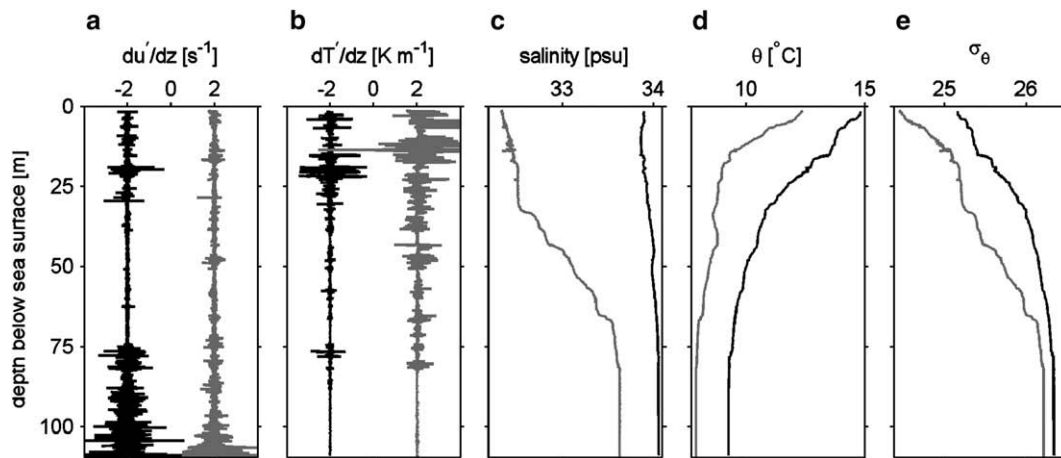


**Fig. 1.** Vertical profiles from opposite sides of Earth but the same depth of water column, one from the Irish Sea, the other from Oregon's continental shelf. a) small-scale velocity shear as detected by shear (or airfoil) probes; b) small-scale temperature gradients detected by fast thermistors—the traces in a), b) have been offset for clarity; c) salinity; d) potential temperature; e) potential density.

that they contribute to an appreciation for the dynamical utility of turbulence measurements in the ocean.

We begin with a brief presentation of raw data that illustrates the variability found in oceanic observations (Section 2). We then review results that show how measurements between groups using similar techniques but which are achieved quite differently in terms of sensor construction, electronics, instrument usage and software processing yield quantitatively similar results (Section 3). This is followed by an example that shows agreement not only between groups but between quite different methods (Section 4) and thence by several examples that clearly establish consistency with the larger scale dynamics (Section 5).

## 2. Examples of ocean turbulence observations

No observation of turbulence in the ocean can be considered typical. However, there are typical characteristics. Profiler observations from the Irish Sea and from Oregon's continental shelf (Fig. 1) display these. Fig. 1a represents the output signal from shear (airfoil) probes that are calibrated to sense small-scale velocity gradients,  $du'/dz$  (Osborn and Crawford, 1980). These reveal large dynamic range in a single profile, associated with the natural variability of high  $Re$  turbulence, represented in spectral representations of geo-

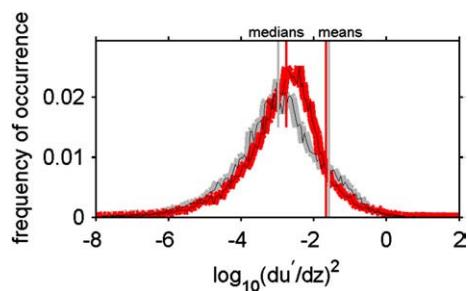


**Fig. 2.** Probability distributions of shear variances derived from each of the two profiles shown in Fig. 1a.

physical turbulence by the large inertial subrange between the energy-containing large scales and the smallest viscous scales (Grant et al., 1962). It is also apparent in probability distributions (Fig. 2) of the variance of the velocity gradients (which is directly proportional to the turbulence dissipation rate,  $\epsilon$ ). Here the small percentage of values in the extended (logarithmic) tails, typical of high kurtosis phenomena, contribute significantly to mean values. The means are nearly two orders of magnitude greater than median values. This caused an unfortunate misuse of the lognormal distribution for prediction of mean oceanic values in the latter part of the twentieth century—the misinterpretation relating to the increased standard deviation of the distribution due to the inclusion of multiple processes with multiple energy sources. For example, in the two profiles shown in Fig. 1, surface mixed layers are separated from bottom boundary layers by stratified thermoclines. So at least two unrelated turbulent fluid processes (forced independently) exist in both profiles. While a lognormal distribution of  $(du'/dz)^2$  may define the individual processes when they are stationary (and on scales smaller than the outer scale of the turbulence; Gurvich and Yaglom (1967)), it does not for the combination.

Another example is seen in data from horizontal tows of turbulence (Fig. 3), here over Oregon's continental slope. In addition to the large variability in small-scale velocity gradients,<sup>1</sup> we note the distinct transition in pattern at about 175 s into the record. The record prior to 175 s is marked by intense patchiness at 5–10 s time scale. After 175 s, the patchiness has considerably diminished. This appears to be related to a transition from possible Kelvin–Helmholtz billows seen in the temperature record (Fig. 3e) prior to 175 s to something else later. In part this indicates the difficulties in

<sup>1</sup> In fact, it is the time derivative rather than the spatial derivative of the velocity that is measured. The spatial derivative is derived assuming Taylor's frozen flow hypothesis. From a vertical profiler, the two components,  $du'/dz$ ,  $dv'/dz$  are derived from probes mounted orthogonally on the profiler's nose. From a towed body, we derive  $dv'/dx$ ,  $dw'/dx$  (Fig. 3g,h).  $z$  is the vertical coordinate direction,  $x$  the direction the towed body moves.

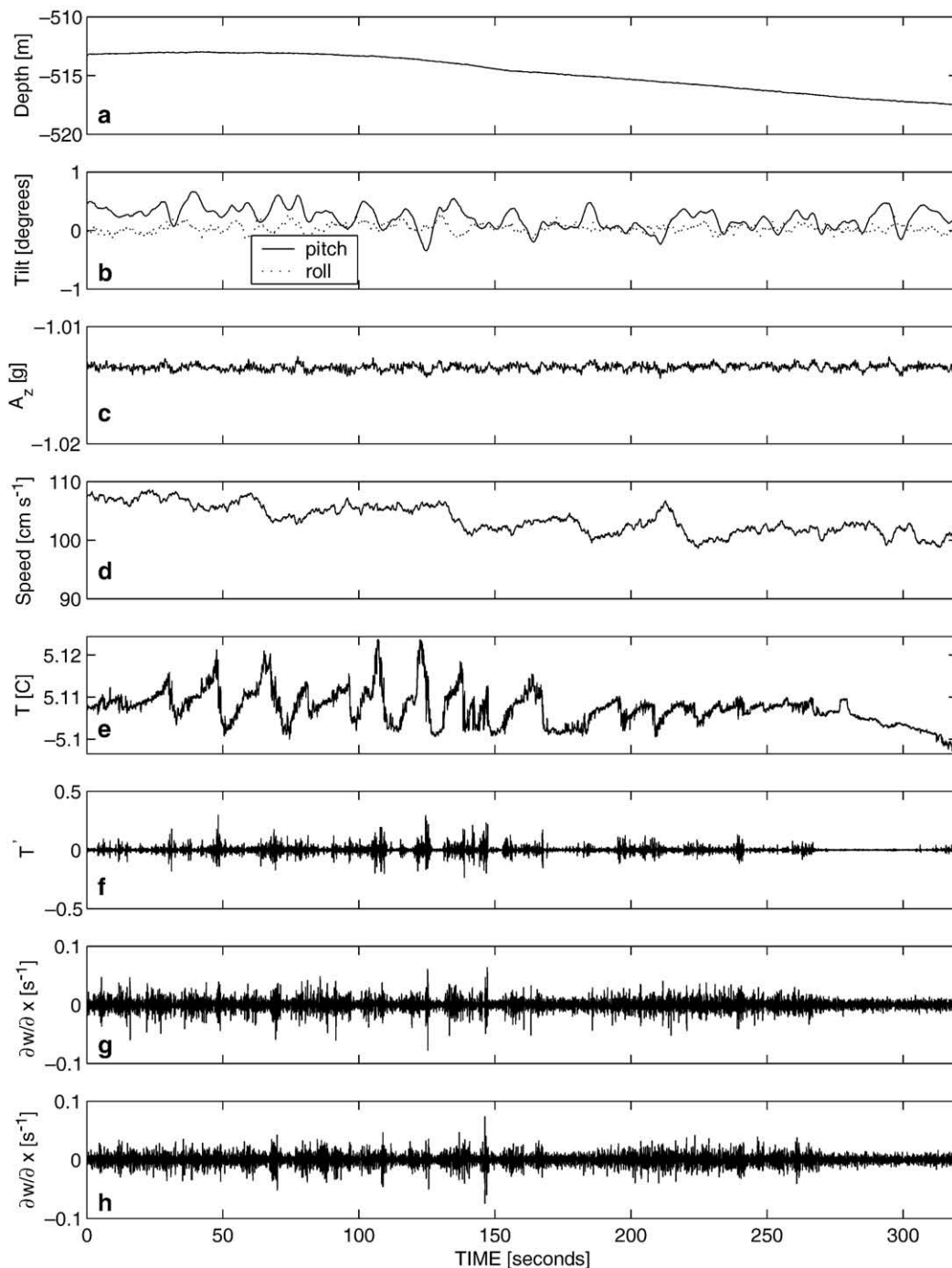


**Fig. 3.** Example data from a horizontal tow using the towed body Marlin at 515 m depth (a) over a 3100 m deep abyssal plain offshore of Oregon's continental slope. The length of this record is 320 s, equivalent to about 320 m at our nominal tow speed of  $1 \text{ m s}^{-1}$  (d); b) body pitch and roll as determined from linear accelerometers; c) vertical acceleration. This is a quiet record. Large values or spikes in  $A_z$  contaminate the turbulence signals and are used as a processing filter; b) flow speed relative to Marlin; e) temperature; f) temperature derivative; g, h) orthogonal signals from two (of three) airfoil probes (Moum et al., 2002).

interpreting turbulence records in the absence of ancillary measurements.

The records shown are typical of those collected by many different groups in a variety of oceanic regimes over the past 40 years. They provide a limited description of the varied ways that turbulence manifests itself in the ocean. The ques-

tion arises whether we can actually use this information in a quantitative manner. We are primarily concerned with meaningful estimation of  $\epsilon$  and turbulence diffusion coefficients  $K_T$ , or  $K_\rho$ . Certainly, the first step in determining whether our measurements of  $\epsilon$  are consistent with what we know about the fundamentals of turbulent flows is to ensure

that wavenumber spectra derived from the measurements can be interpreted in terms of an inertial subrange (Grant et al., 1962) plus an extended viscous subrange such as predicted by the well-founded empirical (Nasmyth, 1970) or theoretical (Panchev and Kesich, 1969) spectra. In fact, we have such faith in these spectral forms, that we consider deviations to indicate problems with the data such as may be caused by hydrodynamically-induced vibrations of the instrument on which sensors are deployed. Many other examples appear in the literature (e.g., Moum et al., 1995).

We assume that the measurements discussed here have passed the test of consistency with known spectral forms and have been vetted for bad data points caused by, for example, zooplankton collisions or shark bites. The issue we address is the reliability of averages derived from the measurements to adequately resolve the natural patchiness and intermittency of oceanic turbulence.

### 3. Intergroup comparisons

Comparative shipboard observations were made at the equator in 1991 during the Tropical Instability Wave Experiment (TIWE). This was a fortunate instance where the attempt to obtain a lengthy time series of turbulence profiling measurements included overlapping ship stays. The resulting 3-day overlap provided an opportunity to compare measurements on both a point-to-point basis and longer term averages (Moum et al., 1995) over a period during which profiling was continuous and the two ships were within a few km of each other. Almost 1000 profiles were obtained from the two

groups, each using its own, and quite different, home-brewed instrumentation, analog signal processing, sensors, calibration procedures and software algorithms. Three significant points arose from this comparison, which is represented in Fig. 4:

- there exists high coherence between time series of  $\epsilon$  at all depths on time scales of a day or so;
- however, there are shorter periods when there are clear, systematic and prolonged differences between the measurements at the two ships. For example, midway through 24 November 1991, one group measured  $\epsilon$  greater by three orders of magnitude at 50 m. At nearly the same time, the same group measured  $\epsilon$  smaller by three orders of magnitude at 125 m. Taken together, these suggest the differences are not artifacts (and in fact, spectral verification tests indicate no reason to think any of the signal to be due to anything but turbulence) but indicate natural variability. Other, though less severe, differences exist in the records;
- over the full 3-day period, averaged vertical profiles agreed within 95% confidence throughout 80% of the water column (Fig. 4e).

The conclusion was that the natural variability was resolved over the period and that any systematic biases between the two independent sets of measurements must be less than a factor of 2.

### 4. Consistency with dye tracer experiments

One of the most significant results from the last decade or so has been the demonstration of enhanced mixing over various

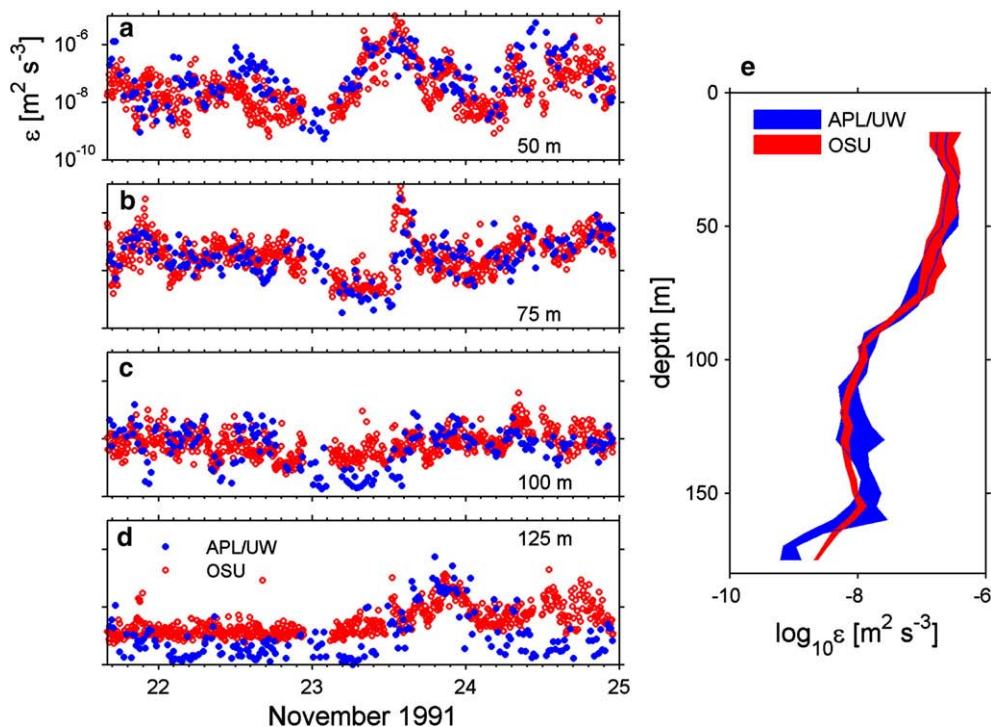


**Fig. 4.** Five-meter vertical averages of  $\epsilon$  from individual profiles obtained at  $0^\circ$ ,  $140^\circ\text{W}$  over a period of 3.5 days in fall 1991. The 203 profiles made by the group from Applied Physics Lab, University of Washington led by Mike Gregg are shown in blue. The 728 profiles obtained by the group from Oregon State University are shown in red. The data are centered at 50 m (a), 75 m (b), 100 m (c) and 125 m (d). Averaged vertical profiles (envelopes of 95% bootstrapped confidence intervals) spanning the full duration (e) (Moum et al., 1995).

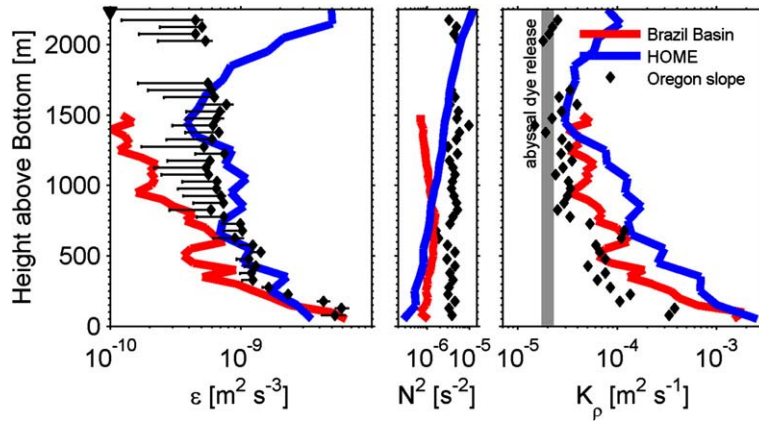


**Fig. 5.** Averaged vertical profiles of  $\epsilon$  (a),  $N^2$  (b) and  $K_\rho$  (c) obtained from vertical profilers in the Brazil Basin (red; Ledwell et al. (2000), Polzin (2004)) and in the Hawaiian Ridge system (blue; Lee et al. (2006)) and from the horizontal profiler, Marlin, over Oregon's continental slope (Moum et al., 2002). The vertical grey bar represents the nominal value determined by dye release experiments in the abyssal ocean away from boundaries (Ledwell et al., 1993).

topographic features, especially in the deep ocean. Aside from the issue of whether or how boundary mixing contributes to the mixing of fluid in the abyssal ocean away from boundaries, there seems to have been confirmed a background value of abyssal mixing of  $K_\rho \approx 2 \times 10^{-5} \text{ m}^2 \text{ s}^{-1}$ . This has come about from quite different measurements covering a range of the world's oceans. Perhaps the most convincing, though, are the dye release measurements that do not measure turbulence at all (Ledwell et al., 1993; Wuest et al., 1996; Ledwell et al., 2000). Rather, they measure start and end states of mixing processes that effect a diapycnal diffusion of the dye. This is an integrated measure of the mixing, not subject to the particular measurement problem of resolving the natural intermittency of the turbulence in the field. Meaningful interpretation requires an adequate accounting of the fate of the dye.

A summary of estimates of  $K_\rho$  determined from measurements of  $\epsilon$  using both vertically- and horizontally-profiling platforms indicates a consistent result where these measurements have been made (Fig. 5). The three sets of results shown come from the Brazil Basin using a vertical profiler in roughly 4500 m water depth (Polzin, 2004), from the Hawaiian Ridge system, again using a vertical profiler where the bottom is referenced to 3000 m depth (Lee et al., 2006). In this case, water depths above 1500 m are affected by other topographic features and in this way differ from the rest. The Oregon slope measurements (Moum et al., 2002) arise from averages at a range of depths from 1600 m to 3100 m depth. By 1000–1500 m above the seafloor, the result seems to be that  $K_\rho$  is not much different from  $2 \times 10^{-5} \text{ m}^2 \text{ s}^{-1}$ , in agreement with the dye estimates.

From these and similar experiments in lakes, Wuest and Lorke (2005) concluded that diffusivity estimates derived from in situ turbulence measurements and from tracer experiments differed by no more than a factor of two.

## 5. Consistency with dynamical constraints

Agreement between research groups (Section 3) and between different methods used to measure mixing (Section 4) is important to establishing a framework for evaluating

measurement techniques and thus helping to develop confidence in the techniques. However, a more severe constraint is defined by the natural laws of physics. That is, the measurements must yield results that are dynamically consistent with the rest of the fluid dynamics. Several examples are instructive.

### 5.1. Interior turbulence stress asymptotes to surface wind stress

If we neglect the contributions of buoyancy flux and advection to the evolution of turbulent kinetic energy, then the mechanical production of turbulence equals that lost to viscous dissipation,

$$P = \epsilon. \quad (1)$$

The definition of an eddy viscosity,  $K_m$  as follows

$$\langle u'w' \rangle = K_m \langle \partial u / \partial z \rangle, \quad \langle v'w' \rangle = K_m \langle \partial v / \partial z \rangle, \quad (2)$$

leads to the observationally derived quantity (Dillon et al., 1989)

$$K_m = \frac{\epsilon}{\langle \partial u / \partial z \rangle^2 + \langle \partial v / \partial z \rangle^2}. \quad (3)$$

We note that inclusion of the buoyancy flux leads to a minor modification to Eq. (3) via a mixing efficiency. With depth profiles of  $\epsilon$  and currents, then, turbulence stress profiles can be constructed. This was done for the three equatorial experiments shown in Fig. 6. These experiments focused on the dominant role thought to be played by turbulence at the equator.<sup>2</sup> An important result from this comparison is that, while there is, considerable variability in the structure and magnitude of the turbulence stress, in each case, the turbulence stress roughly asymptotes to the local value of the surface wind stress, as it must.

<sup>2</sup> As it has turned out, the contribution to the divergence of the momentum stress due to locally-generated and vertically-propagating internal waves may sometimes be greater.

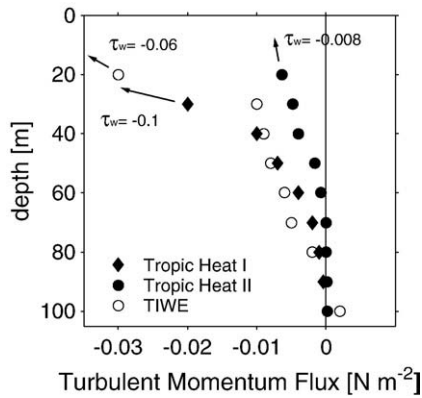


**Fig. 6.** Turbulent momentum flux profiles taken at the same equatorial location (0°, 140°W) in 1984 (TROPIC HEAT I; Dillon et al. (1989)), 1987 (TROPIC HEAT II; Hebert et al. (1991)) and in 1991 (Tropical Instability Wave Experiment, TIWE; Lien et al. (1995)).  $\tau_w$  refers to the surface wind stress at the time of each set of observations.

5.2. Surface-driven convection

Another example arises from times when the upper ocean (or lake) is primarily forced by cooling of the surface. This occurs regularly at nighttime (Imberger, 1985; Shay and Gregg, 1986; Anis and Moum, 1994) and when cold air outbreaks appear over warm water (Shay and Gregg, 1986). This situation is analogous to the atmospheric mixed layer when it is heated from below during the daytime (Caughey and Palmer, 1979). When convection occurs, the mixed layer (separated from the surface by a stress-driven surface layer) is forced primarily by the surface buoyancy flux,  $J_b^0$ , rather than  $P$ . A summary of results (Fig. 7) clearly shows the agreement that has arisen from very different types of experiments in the ocean (Shay and Gregg, 1986; Anis and Moum, 1994), lakes (Imberger, 1985) and atmospheric boundary layers (Caughey and Palmer, 1979) in both Minnesota and Australia.

In detail, the average structure of  $\epsilon(z)$  shows it to be linear (Anis and Moum, 1994), implying that the buoyancy (and heat) flux is linear, as well. This is in agreement with other constraints on the turbulent heat flux profile (Anis and Moum, 1994).

5.3. Nonlinear internal wave energy losses

Recent experiments designed to track large amplitude, highly nonlinear internal waves over continental shelves indicate that once the waves have become relatively solitary and separated from the bores that appear to be their progenitors, a simple balance emerges (Moum et al., 2007). That is, the energy lost by the wave is nearly exactly accounted for by losses to turbulence,

$$\langle \frac{dE_w}{dt} \rangle = -\langle \rho \epsilon \rangle, \tag{4}$$

where  $\langle \rangle$  represents a cross-sectional average of the wave. This balance appears to hold over propagation distances of hundreds of wavelengths as the waves feel the bottom but before they are seriously deformed by it and in the absence of

other wave interactions which can radically alter the balance over short time scales.

5.4. Tidal dissipation in shelf seas

A major step forward in our understanding of tides in continental shelf seas came through the work of G.I. Taylor in his study of the Irish Sea (Taylor, 1919). He showed that the direct astronomical forcing of the tide in this shelf sea is negligible and so the rate at which energy is being dissipated within a basin should approximate to the net flux of tidal energy into the basin. Assuming all of the energy is dissipated through bed shear stresses, based on a quadratic drag law.

$$E_{\text{tide}} = \int_{\text{bbf}} \rho \epsilon = C_d \rho U |u|^2. \tag{5}$$

Taylor was able to show that the total basin dissipation rate balanced the flux of energy into the basin, taking a value of  $C_d=0.002$ . Subsequent numerical modeling studies of various shelf seas, which employ the quadratic friction law in order to account for friction in the system, have accurately reproduced the barotropic tide taking values of  $C_d$  in the range 0.0015–0.0025 (Bowers et al., 1991).

At the same time, oceanic environments where the local kinetic energy budget is dominated by the tide provide an ideal location for testing of equipment for the measurement of marine turbulence in comparison to more easily obtained variables such as sea level height or tidal currents. Tides provide a predictable and cyclical signal on timescales of a day, which are adequately sampled at relatively low resolution (order 10 min) over periods easily manageable for manually operated equipment such as loosely tethered microstructure profilers.

As a check on the accuracy of the observed dissipation we might thus compare the water column integrated dissipation with the estimate based on the quadratic drag law. This was

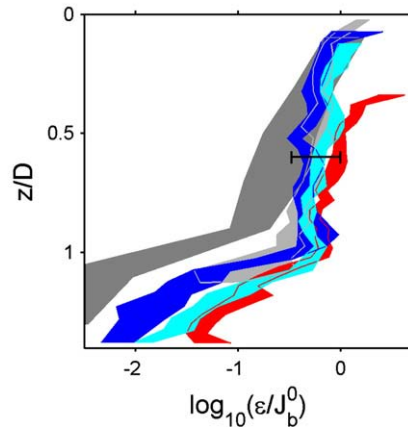
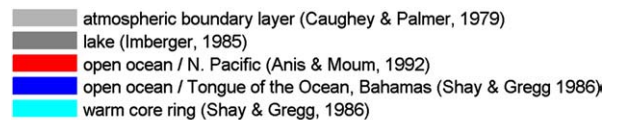


**Fig. 7.** Nondimensionalized profiles of  $\epsilon$  obtained in very different geophysical flows and measured in a variety of ways. Depth ( $z$ ) is scaled by the mixed layer depth  $D$ .  $\epsilon$  is scaled by the surface value of the buoyancy flux, ( $J_b^0$ ). The horizontal bar represents a factor of 2.

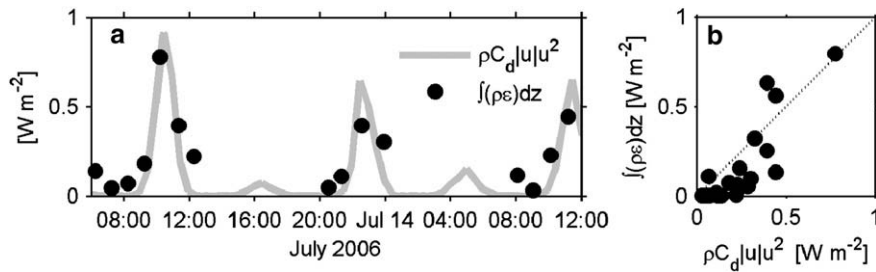


**Fig. 8.** a) Time series of depth integrated turbulence dissipation ( $\int(\rho\varepsilon)dz$ ) from profiler measurements together with an estimate of the BBL dissipation based on a quadratic drag law ( $\rho C_d |u|u^2$ ) using 30 min velocity averages from an acoustic Doppler current profiler measurement 10 m above the bed and  $C_d=0.0025$ . These measurements were made at a neutrally-stratified site to the north east of Anglesey where the water depth is 40 m and the sea bed is flat and sandy. b) Scatter plot showing the correspondence between measured dissipation and the quadratic drag law estimate.

nicely shown by Dewey and Crawford (1988) and repeated elsewhere in various forms (Simpson et al., 1996; Stacey et al., 1999; Rippeth et al., 2002; Perlin et al., 2005). In Fig. 8 is shown a recent comparison.

### 5.5. Bottom boundary layers

In neutrally-stratified bottom boundary layers, it is reasonable to consider that Eq. (1) holds, at least away from the immediate seafloor and the stratified cap of the bottom boundary layer, where advection of turbulence kinetic energy is significant. Using data collected in Red Wharf Bay, off the north coast of Anglesey, Rippeth et al. (2003) and Wiles et al. (2006) compare profiles of  $\varepsilon$  from velocity microstructure and

applying a structure function technique to ADCP velocity profiles, and estimates of the rate of production of TKE using the ADCP variance technique. The results (Fig. 9) show reasonable agreement between the three techniques, with the ratios  $\varepsilon_{sf}/\varepsilon_{FLY}=0.68\pm 0.23$  and  $\varepsilon_{FLY}/P=0.63\pm 0.17$ . The water depth at the measurement site varied between 19 m at low water to 25 m at high water, and there is a rectilinear tidal flow with maximum currents reaching  $1\text{ ms}^{-1}$ .

### 6. Synopsis

Early microstructure measurements at depth (Gregg, 1977; Moum and Osborn, 1986) showed a diapycnal diffusivity which was about an order of magnitude less than the

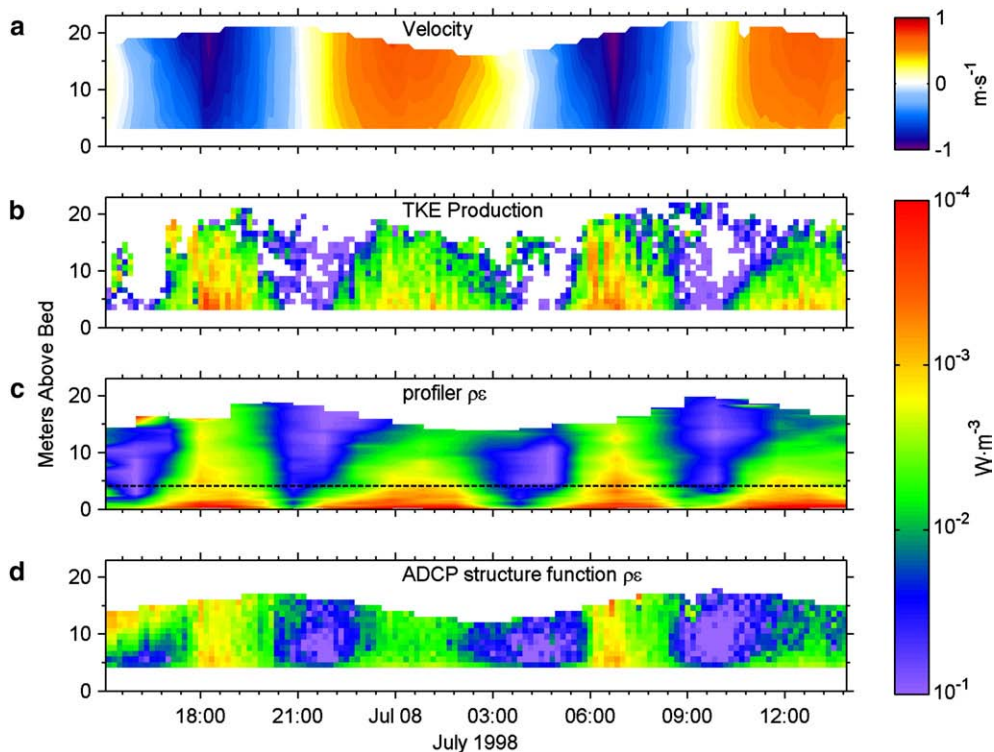


**Fig. 9.** Time evolution of profiles of (a) along stream velocity, (b) shear production rate of TKE using the ADCP variance method, (c) TKE dissipation rate from a loosely tethered profiler and (d) TKE dissipation rate using a structure function technique applied to ADCP velocity data. The data was collected in a neutrally-stratified water column in Red Wharf Bay, North Wales.

canonical value estimated from tracers using inverse models,  $10^{-4} \text{ m}^2 \text{ s}^{-1}$  (Munk, 1966). It was reasonably speculated, at that time, that microstructure measurements were not giving correct estimates of the magnitudes of turbulence diffusion coefficients. However, more recent open ocean dye-diffusion experiments confirmed the earlier microstructure estimates (Ledwell et al., 1993) and this has been further buttressed by other experiments using various sensor platforms (some of which are represented in Fig. 5). In answer to the title question, then, we conclude that turbulence measurements, when made in a reasonably comprehensive and systematic manner and properly screened for data quality, are providing significant quantitative insights into ocean dynamics.

Our conclusion may seem at odds with that expressed recently by Ivey et al. (2008), who state

‘we conclude that our sampling and interpretation of the results remain a first-order issue, and despite decades of ship-based observations we do not approach a reliable sampling of the overall turbulent structure of the ocean interior.’

We are in agreement that we are a long way from achieving an understanding of the global geography and time dependence of mixing, especially on long time scales. Aside from this, the above conclusion was reached from the perspective of numerical simulations and laboratory experiments, which have suggested the potential for misinterpretation of microstructure flux formulations due to the spatial heterogeneity and temporal evolution of controlled and isolated patches of turbulence studied in simulations and laboratory flows. A reassessment of thermocline estimates of mixing efficiency  $\Gamma$  (Moum, 1996) by Smyth et al. (2001) suggested a 50–60% increase in median diffusivity when a diagnostic clock defined from simulations to represent the time dependence of  $\Gamma$  is applied to the oceanic observations. From the perspective of observationalists who rarely have the luxury of evaluating controlled and isolated patches of turbulence, we have always considered a factor of two to be an achievement.

To date, measurements of turbulence in the ocean have been most effectively made from shipborne sensor platforms. These have led to first-order advances in our understanding of processes that can be easily sampled over the duration of a seagoing experiment and sampled synoptically at ship speeds. There is now considerable interest in extending turbulence measurements to moored and AUV platforms, thereby both expanding the exploratory role of turbulence measurements and extending sampling periods to annual and longer time scales. Acoustic techniques present particularly exciting opportunities, although may be limited by power consumption. New, low power devices to measure mixing are in development and results will soon be broadly reported.

## Acknowledgements

This paper arose from the 2007 Liege Colloquium on Ocean Dynamics: ‘Turbulence Re-Visited’. We are grateful to the chief organizers, Hans Burchard and Jean-Marie Beckers, for their efforts in providing a rich learning experience for participants. Two anonymous reviewers

offered constructive suggestions. JNM has been funded by the US Office of Naval Research and the National Science Foundation (0424133). TPR has been funded by the Natural Environment Research Council of the UK.

## References

- Anis, A., Moum, J.N., 1994. Prescriptions for heat flux and entrainment rates in the upper ocean during convection. *J. Phys. Oceanogr.* 24, 2142–2155.
- Bowers, D.G., Rippeth, T.P., Simpson, J.H., 1991. Tidal friction in a sea with two equal semidiurnal tidal constituents. *Cont. Shelf Res.* 11, 203–209.
- Caughey, S.J., Palmer, S.G., 1979. Some aspects of turbulent structure through the depth of the convective boundary layer. *Quart. J. Roy. Meteor. Soc.* 105, 811–827.
- Dewey, R.K., Crawford, W.R., 1988. Bottom stress estimates from vertical dissipation rate profiles on the continental shelf. *J. Phys. Oceanogr.* 18, 1167–1177.
- Dillon, T.M., Moum, J.N., Chereskin, T.K., Caldwell, D.R., 1989. Zonal momentum balance at the equator. *J. Phys. Oceanogr.* 19, 561–570.
- Grant, H.L., Stewart, R.W., Moilliet, A., 1962. Turbulence spectra in a tidal channel. *J. Fluid Mech.* 12, 241–268.
- Gregg, M.C., 1977. Variations in the intensity of small scale mixing in the main thermocline. *J. Phys. Oceanogr.* 7, 436–454.
- Gurvich, A.S., Yaglom, A.M., 1967. Breakdown of eddies and probability distributions. *Phys. Fluids* 10, S59–S65.
- Hebert, D., Moum, J.N., Paulson, C.A., Caldwell, D.R., Chereskin, T.K., McPhaden, M.J., 1991. The role of the turbulence stress divergence in the equatorial Pacific zonal momentum balance. *J. Geophys. Res.* 96, 7127–7136.
- Imberger, J., 1985. The diurnal mixed layer. *Limnol. Oceanogr.* 30, 737–770.
- Ivey, G.N., Winters, K.B., Koseff, J.R., 2008. Density stratification, turbulence, but how much mixing? *Ann. Rev. Fluid Mech.* 40, 169–184.
- Ledwell, J.R., Watson, A.J., Law, C.S., 1993. Evidence for slow mixing across the pycnocline from an open-ocean tracer-release experiment. *Nature* 364, 701–703.
- Ledwell, J.R., Montgomery, E.T., Polzin, K.L., St. Laurent, L.C., Scmitt, R.W., Toole, J.M., 2000. Evidence of enhanced mixing over rough topography in the abyssal ocean. *Nature* 403, 179–182.
- Lee, C.M., Kunze, E., Sanford, T.B., Nash, J.D., Merrifield, M.A., Holloway, P.E., 2006. Internal tides and turbulence along the 3000-m isobath of the Hawaiian Ridge. *J. Phys. Oceanogr.* 36, 1165–1183.
- Lien, R.C., Caldwell, D.R., Gregg, M.C., Moum, J.N., 1995. Turbulence variability in the central equatorial Pacific at the beginning of the 1991–1993 El Niño. *J. Geophys. Res.* 100, 6881–6898.
- Moum, J.N., 1996. Efficiency of mixing in the main thermocline. *J. Geophys. Res.* 101 (C5), 12,057–12,069.
- Moum, J.N., Osborn, T.R., 1986. Mixing in the main thermocline. *J. Phys. Oceanogr.* 16, 1250–1259.
- Moum, J.N., Gregg, M.C., Lien, R.C., Carr, M.E., 1995. Comparison of turbulent kinetic energy dissipation rates from two ocean microstructure profilers. *J. Atmos. Ocean. Technol.* 12, 346–366.
- Moum, J.N., Caldwell, D.R., Nash, J.D., Gunderson, G.D., 2002. Observations of boundary mixing over the continental slope. *J. Phys. Oceanogr.* 32, 2113–2130.
- Moum, J.N., Farmer, D.M., Shroyer, E.L., Smyth, W.D., Armi, L., 2007. Dissipative losses in nonlinear internal waves propagating across the continental shelf. *J. Phys. Oceanogr.* 37, 1989–1995.
- Munk, W.H., 1966. Abyssal recipes. *Deep-Sea Res.* 13, 707–730.
- Nasmyth, P., 1970. Oceanic turbulence, Ph.D. thesis, University of British Columbia, 69 pp.
- Osborn, T.R., Crawford, W.R., 1980. An airfoil probe for measuring turbulent velocity fluctuations in water. In: Dobson, F., Hasse, L., Davis, R. (Eds.), *Air–Sea Interaction: Instruments and Methods*. Plenum, pp. 369–386.
- Panchev, S., Kesich, D., 1969. Energy spectrum of isotropic turbulence at large wavenumbers. *Compt. Rend. Acad. Bulgare. Sci.* 22, 627–630.
- Perlin, A., Moum, J.N., Klymak, J.M., Levine, M.D., Boyd, T., Kosro, P.M., 2005. A modified law-of-the-wall applied to oceanic bottom boundary layers. *J. Geophys. Res.* 110. doi:10.1029/2004JC002310.
- Polzin, K.L., 2004. Idealized solution for the energy balance of the finescale internal wave field. *J. Phys. Oceanogr.* 34, 231–246.
- Pope, S.B., 2000. *Turbulent Flows*. Cambridge, 771 pp.
- Rippeth, T.P., Williams, E., Simpson, J.H., 2002. Reynolds stress and turbulent energy production in a tidal channel. *J. Phys. Oceanogr.* 32, 1242–1251.
- Rippeth, T.P., Simpson, J.H., Williams, E., Inall, M.E., 2003. Measurements of the rates of production and dissipation of turbulent kinetic energy in a energetic tidal flow. *J. Phys. Oceanogr.* 33, 1889–1901.
- Shay, T.J., Gregg, M.C., 1986. Convectively-driven turbulence in the upper ocean. *J. Phys. Oceanogr.* 16, 1777–1797.

- Simpson, J.H., Crawford, W.R., Rippeth, T.P., Campbell, A.R., Cheok, J.V.S., 1996. The vertical structure of turbulent dissipation in shelf seas. *J. Phys. Oceanogr.* 26, 1579–1590.
- Smyth, W.D., Moum, J.N., 2001. Three-dimensional (3D) turbulence, *Encyclopedia of Ocean Sciences*. Academic Press.
- Smyth, W.D., Moum, J.N., Caldwell, D.R., 2001. The efficiency of mixing in turbulent patches: inferences from direct simulations and microstructure observations. *J. Phys. Oceanogr.* 31, 1969–1992.
- Stacey, M.T., Monismith, S.G., Burau, J.R., 1999. Observations of turbulence in a partially stratified estuary. *J. Phys. Oceanogr.* 29, 1950–1970.
- Taylor, G.I., 1919. Tidal Friction in the Irish Sea. *Phil. Trans. Roy. Soc. A*, vol. ccxx, pp. 1–93.
- Thorpe, S.A., 2005. *The Turbulent Ocean*. Cambridge. 439 pp.
- Wiles, P.J., Rippeth, T.P., Simpson, J.H., Hendricks, P.J., 2006. A novel technique for measuring the rate of turbulence dissipation in the marine environment. *Geophys. Res. Lett.* 33, L21608. doi:10.1029/2006GL027050.
- Wuest, A., Lorke, A., 2005. Validation of microstructure-based diffusivity estimates using tracers in lakes and oceans. In: Baumert, H., Simpson, J., Sundermann, J. (Eds.), *Marine Turbulence: Theories, Observations and Models*. Results of the CARTUM Project. Cambridge University Press, pp. 139–152.
- Wuest, A., van Senden, D.C., Imberger, J., Piepke, G., Gloor, M., 1996. Comparison of diapycnal diffusivity measured by tracer and microstructure techniques. *Dyn. Atmos. Ocean.* 24, 27–39.